

Controlling absorption resonances from sub-wavelength cylinder arrays

Marine Laroche,¹ Raquel Gómez-Medina,² and Juan José Sáenz¹

¹*Departamento de Física de la Materia Condensada and Instituto “Nicolás Cabrera”,
Universidad Autónoma de Madrid, E-28049 Madrid, Spain.**

²*Nanophotonics and Metrology Laboratory,
Swiss Federal Institute of Technology, 1015 Lausanne, Switzerland*

(Dated: 24, April 2006)

Abstract

The absorption and extinction spectra of sub-wavelength cylinder arrays are shown to present two different kind of resonances. Close to the Rayleigh anomalies, the diffractive coupling with the lattice periodicity leads to sharp peaks in the extinction spectra with characteristic Fano line shapes for both s and p -polarizations. When the material exhibits an absorption line or in the presence of localized surface plasmon/polaritons, the system is shown to present resonant absorption with wider and symmetric line shapes. For s -polarization our analysis predict a theoretical limit of 50% of absorption. Interestingly, for p -polarized light and an appropriate choice of parameters, a subwavelength cylinder array can present perfect (100%) absorption.

PACS numbers: 42.25.Bs,42.79.Dj,44.40.+a,73.20.Mf

The study of the extinction spectra of nanoparticles have drawn much attention recently for their potential applications to chemical and biological sensors as well as for Surface Enhanced Raman Scattering (SERS) [1–3]. While for a single nanoparticle, the excitation of localized surface plasmon/polariton resonances (LSPR) lead to well defined extinction line shapes at specific wavelengths[2], for an assemble of nanoparticles the spectra can be substantially modified by multiple scattering effects. For absorbing materials, resonant *radiative* diffraction as well as resonant *absorption* processes could both lead to sharp peaks in the extinction spectra. Our main purpose is to understand the relative role of both processes in the spectra of nanoparticle arrays. This is an important issue from a fundamental point of view but it is also specially relevant for a wide range of applications: By Kirchhoff’s law [4], the control of absorption by nanostructured materials is equivalent to tailor the thermal emission. This is of interest for thermophotovoltaic applications and for the design of efficient infrared sources. The recent development of coherent thermal sources [5, 6] has stimulated further work on thermal emission from photonic crystals [7–9] or nanoparticle arrays [10].

In the visible range, plasmon resonances on linear array of metallic particles have been intensively studied considering the influence of different parameters on the extinction spectra [11–13]. Enhanced absorption by dielectric particles resulting of phonon-polariton resonances has also been demonstrated in the infrared [14]. Peaks in the extinction spectra are commonly associated to the excitation of LSPR modified by the diffractive coupling with the lattice periodicity [13, 14]. For cylinder arrays, *s*-polarized electromagnetic radiation (with the electric field parallel to the cylinder axis) can not excite any surface plasmon. However, the extinction spectra of subwavelength cylinder arrays of non-absorbing dielectric materials present sharp peaks even for *s*-polarization [15].

In this letter, we study the extinction spectra of sub-wavelength cylinder arrays. As we will see, the spectra present two different kind of resonances. Close to the Rayleigh anomalies, the diffractive coupling with the lattice periodicity leads to sharp peaks in the extinction spectra with characteristic Fano line shapes for both *s* and *p*-polarizations. These *geometric* resonances, associated to radiative coupling in absence of absorption, may lead to resonant absorption for appropriate grating parameters. We analytically derive the conditions for resonant absorption as a function of the geometry and material’s parameters. Another kind of absorption resonances, with wider and symmetric line shapes, appears when the material

exhibits an absorption line or in the presence of LSPRs. In contrast with geometric resonances, these absorption peaks are almost isotropic with a weak dependence on the angle of incidence and geometry. We will demonstrate that for s -polarization there is a theoretical limit of 50% of absorption. Interestingly, we will show that, for p -polarized light and an appropriate choice of parameters, a subwavelength cylinder array can present perfect (100%) absorption.

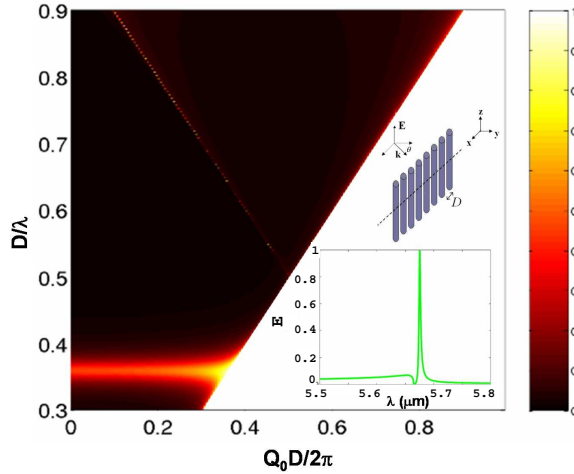


FIG. 1: (s -**polarization**) Extinction in s -polarization in a map of frequency (D/λ) versus the transversal momentum of the incoming radiation ($Q_0 = 2\pi \sin \theta/\lambda$), for an array of SiC nanocylinders with period $D = 4.5\mu\text{m}$ and radius $a = 0.2\mu\text{m}$. Around $D/\lambda = 0.36$ ($\lambda = 12.5\mu\text{m}$), there is an isotropic extinction peak due to the absorption line of SiC. The inset shows the extinction spectrum, which exhibits a typical Fano line shape, for an incident angle $\theta = 15^\circ$ around the geometric resonance (close to the first Rayleigh frequency, i.e. $D/\lambda = 1 - Q_0 D/2\pi$).

Let us consider an infinite set of parallel cylinders with their axis along the z -axis (see inset in Fig. 1), relative dielectric constant $\epsilon = \epsilon' + i\epsilon''$ and radius a much smaller than the wavelength. The cylinders are located at $\mathbf{r}_n = nD\mathbf{u}_x = x_n\mathbf{u}_x$ (with n an integer number). For simplicity, we will assume incoming plane waves with wave vector $\mathbf{k}_0 \perp \mathbf{u}_z$ (i.e. the fields do not depend on the z -coordinate), with $k = \omega/c$ and $\mathbf{k}_0 = k \sin \theta \mathbf{u}_x + k \cos \theta \mathbf{u}_y \equiv Q_0 \mathbf{u}_x + q_0 \mathbf{u}_y$. The reflectance, R and transmittance, T of the cylinder array can be calculated by using a standard multiple scattering approach in the dipolar approximation [16], as described in Ref. [15]. We define the absorptivity, A , as: $A \equiv 1 - R - T$ and the normalized extinction, E , as the ratio between scattered plus absorbed powers and incoming power (notice that,

below the onset of the first diffraction beam, the extinction is simply given by the sum of absorption and specular reflection, $E = A + R$).

Let us first consider the simpler case of *s*-polarized electromagnetic waves. For a single sub-wavelength cylinder, the polarizability is given by

$$\frac{1}{k^2 \alpha_{zz}} = \{C(\epsilon' - 1) + \dots\} - i \left\{ \frac{1}{4} + C\epsilon'' + \dots \right\} \quad (1)$$

where $C^{-1} \equiv \pi(ka)^2|\epsilon - 1|^2$. It is worth noticing that $(-\Im\{1/(k^2 \alpha_{zz})\} - \frac{1}{4}) \propto \epsilon''$, so, in absence of absorption ($\epsilon'' = 0$), the expression above is consistent with the optical theorem [15, 17, 18]. Multiple scattering effects, due to the presence of the other scatterers, can be included in a renormalized polarizability, $\hat{\alpha}_{zz}$ [15, 17]. Generalizing the results of Ref. [15] to include absorption we find

$$(k^2 \hat{\alpha}_{zz})^{-1} = \Re \left\{ \frac{1}{k^2 \alpha_{zz}} - G_b \right\} - i \{C\epsilon'' + \Im\{G\}\} \quad (2)$$

where G_b is the depolarization term [15, 17, 19], defined as $G_b = \lim_{\mathbf{r} \rightarrow \mathbf{r}_0} [G(\mathbf{r}) - G_0(\mathbf{r}, \mathbf{r}_0)]$, being G and G_0 the Green function of the periodic array and the free-space respectively, and $\Im\{G\} \equiv \Im\{G(0)\}$. The absorptivity and normalized extinction can now be written in terms of $\hat{\alpha}_{zz}$ as:

$$A^{(s)} = \frac{k^4 |\hat{\alpha}_{zz}|^2}{Dq_0} C\epsilon'' \quad (3)$$

$$E^{(s)} = A^{(s)} + \frac{k^4 |\hat{\alpha}_{zz}|^2}{Dq_0} \left(\Im\{G\} - \frac{1}{4Dq_0} \right). \quad (4)$$

In order to illustrate the main physics involved in the different resonant phenomena, we will consider a typical dielectric constant given by: $\epsilon = \epsilon_\infty (\omega_L^2 - \omega^2 - i\gamma\omega) \{\omega_T^2 - \omega^2 - i\gamma\omega\}^{-1}$. This is a standard form for a polar material (Lorentz model), for a metal, the Drude model is recovered taking $\omega_T = 0$ and $\omega_L = \omega_p$. Silicon carbide (SiC) nanowires provide a simple model system: its dielectric constant is given by this form with the following parameters [20]: $\epsilon_\infty = 6.7$, $\omega_L = 1.825 \cdot 10^{14}$ rad.s⁻¹, $\omega_T = 1.494 \cdot 10^{14}$ rad.s⁻¹, $\gamma = 8.9662 \cdot 10^{11}$ rad.s⁻¹. Figure 1 displays the extinction in the infrared range, in a map of frequency (D/λ) versus the transversal momentum of the incoming radiation (Q_0), for an array of SiC cylinders (with $D = 4.5 \mu\text{m}$ and $a = 0.2 \mu\text{m}$). The extinction spectra show two different kinds of resonances: *i*) close and below the Rayleigh frequency $\omega \rightarrow \omega_1^{(-)} = c|Q_0 - 2\pi/D|$ the spectra present a very sharp peak with a

strong dependence on the angle of incidence, and *ii*) a broad peak close to the absorption line of SiC ($\omega \approx \omega_T$) which is almost isotropic. The peaks in the extinction spectra correlate with corresponding maxima in the absorption. However, the relative strength of the peaks depends on the material and geometrical parameters. This is illustrated in Fig.2 where we have plotted the real part of $1/\alpha_{zz}$ and the imaginary parts of α_{zz} (2a), the absorptivity (2b) and the extinction (2c) versus the wavelength for an incident angle $\theta = 15^\circ$ and for different lattice constants, D (the inset in Fig. 1 corresponds to a zoom of the bold solid line in Fig. 2c).

The different extinction/absorption resonances resemble the recently discussed “lattice” [15, 21] and “site” [22] resonances in absence of absorption. Resonant processes arise when the real part of $1/(k^2\alpha_{zz}) - G_b$ vanishes. Approaching the threshold of the first propagating (diffraction) channel, the real part of G_b goes to infinity as $\approx (\omega_1^2 - \omega^2)^{-1/2}c/(2D)$ and can compensate exactly the real part of $1/k^2\alpha_{zz}$ giving rise to a “geometric” resonance [15, 17]. This can only happen when the real part of the polarizability is positive ($\epsilon' > 1$). As a consequence, in *s*-polarization there is no resonant absorption for metallic cylinders. The typical Fano line shape of these resonances is illustrated in the inset of Fig. 1. While it is possible to obtain a 100% extinction of the beam (due to the reflection resonances which appear when the absorption is weak [15]), the maximum absorption A_{max} is limited to a 50 % (see Fig.2(b,c)). It is easy to show that the highest absorption, $A_{max} = 1/2$, takes place below the first Rayleigh frequency when

$$C\epsilon'' = \frac{\epsilon''}{\pi(ka)^2|\epsilon - 1|^2} = \frac{1}{2Dq_0}. \quad (5)$$

This is one of the central results of this work. We can also notice that at the Rayleigh frequency, $\omega = \omega_1$, the array of cylinders is transparent as the absorption and the extinction goes to zero.

Material or “site” resonances are associated to the zeros of the real part of $1/\alpha_{zz}$. As shown in Fig.2(a), it exhibits two zeros, one close to $\omega \simeq \omega_T$ the other to $\omega \simeq \omega_S = (\epsilon_\infty\omega_L^2 - \omega_T^2)/(\epsilon_\infty - 1)$. The second one corresponds to a small value of $\Im\{\alpha_{zz}\}$, which leads to a weak absorption. The broad resonances in Figure 2(b) and (c) coincide with a maximum of $\Im\{\alpha_{zz}\}$ and correspond to a resonant absorption of the material. Then, they should not be very sensitive to the lattice parameters and order. However, the maximal absorptivity value of 1/2 can only be reached at the condition given by eq. 5. Close to the Rayleigh

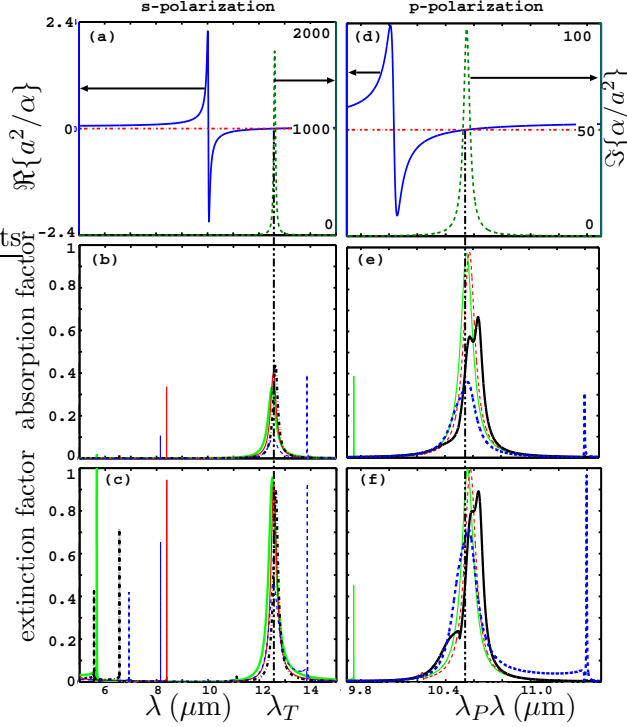


FIG. 2: (*s*-polarization) (a): Real part of $1/\alpha_{zz}$ (-) and imaginary part of α_{zz} (- -) versus λ for SiC cylinders. Absorption resonance is due to a zero ($-\cdot-$) of $\Re\{1/\alpha_{zz}\}$, which coincides with a maximum of $\Im\{\alpha_{zz}\}$. (b): Absorption spectrum versus λ for arrays of cylinder of radius $a = 0.2 \mu\text{m}$, for an incident angle $\theta = 15^\circ$ and for several periods $D = 4.5 \mu\text{m}$ (green bold solid line), $D = 6.67 \mu\text{m}$ (red solid line), $D = 8.83 \mu\text{m}$ (black dotted-dash line), $D = 11 \mu\text{m}$ (blue dashed line). (c): Extinction spectrum for the same parameters than (b).

(*p*-polarization) (d): Real part of $1/\alpha_p$ (-) and imaginary part of α_p (- -) versus λ for SiC cylinders. (e): Absorption spectrum versus λ for arrays of cylinders of radius $a = 0.5 \mu\text{m}$ and different periods $D = 5.71 \mu\text{m}$ (green solid line), $D = 6.0 \mu\text{m}$ (red dashed line), $D = 6.15 \mu\text{m}$ (black bold solid line), $D = 6.667 \mu\text{m}$ (blue bold dashed line), (f): Extinction spectrum for the same parameters than (e).

frequencies, there is a small blue or red-shifted depending of the value of the real part of G_b (see Fig 2a. of ref [15]).

Let us now consider an incoming wave with the magnetic field parallel to the cylinder axis (*p*-polarized wave). Following the notation of ref. [15] we can now define the renormalized polarizabilities of the effective dipoles pointing along the x and y axis:

$\hat{\alpha}_{xx} = (1 + \alpha_{xx}\partial_y^2 G_b)^{-1} \alpha_{xx}$, $\hat{\alpha}_{yy} = (1 + \alpha_{yy}\partial_x^2 G_b)^{-1} \alpha_{yy}$, being $\partial_{x,y}^2 G_b$ the depolarization terms due to the components x and y of the electric field scattered by all the dipoles (except the considered one) and $\alpha_{xx} = \alpha_{yy} = \alpha_p$ the polarizability of a cylinder in p-polarization,

$$\frac{1}{k^2 \alpha_p} = \left\{ \frac{C}{2} (|\epsilon|^2 - 1) + \dots \right\} - i \left\{ \frac{1}{8} + C\epsilon'' + \dots \right\}. \quad (6)$$

The general expression for the absorption is:

$$A^{(p)} = \frac{k^2}{Dq_0} (Q_0^2 |\hat{\alpha}_{yy}|^2 + q_0^2 |\hat{\alpha}_{xx}|^2) C\epsilon''. \quad (7)$$

Hence, in p-polarization, the absorption results from the sum of the contributions of two dipoles, one pointing in the x-direction (with an effective polarizability $\hat{\alpha}_{xx}$) and one pointing in the y-direction (with an effective polarizability $\hat{\alpha}_{yy}$).

At the threshold of the first propagating order, there is a resonant coupling of electric dipoles pointing along the y -axis which leads to the divergence of $\Re\{\partial_x^2 G_b\} \approx -(\omega_1^2 - \omega^2)^{-1/2} \omega_1^2 / (2cD)$ at the Rayleigh frequencies (in contrast $\Re\{\partial_y^2 G_b\}$ remains finite). Close to the first Rayleigh anomaly ($\omega \lesssim \omega_1$) and providing that $\Re\{1/\alpha_p > 0\}$ [15], the absorption contains two parts: a resonant part due to the resonance of $\hat{\alpha}_{yy}$ (and similar to the case in s-polarization), and the term due to $\hat{\alpha}_{xx}$ to which we will refer as a "background contribution". For p-polarization, the resonant part has also a maximal value of 1/2 and reaches this maximum when

$$C\epsilon'' = \frac{Q_0^2}{k^2} \frac{1}{2Dq_0}. \quad (8)$$

Depending on the contribution of the non-resonant part, the absorption can reach a value higher than 1/2.

Site resonances for p-polarization are again associated to zeros of the real part of $1/\alpha_{xx} = 1/\alpha_{yy} = 1/\alpha_p$. $\Re\{1/\alpha_p\}$ exhibits two zeros (see Fig. 2 (d)): one close to $\omega \simeq \omega_S$, but corresponding to a small value of $\Im\{\alpha_p\}$ and to $\epsilon' = +1$ and thus a weak absorption (for SiC, $\lambda_S = 10.0\mu m$), the other close to $\omega \simeq \omega_P$ ($\epsilon' \approx -1$) which gives rise to (phonon-polaritons or plasmon-polaritons for metals) LSPR (for SiC, $\lambda_P = 10.57\mu m$). In contrast with the geometric resonances, the LSPR will lead to the resonance of both dipoles. As each dipole can contribute up to 1/2, the absorption may reach 100%.

We have to notice that unless $\Re\{\partial_x^2 G_b\} = \Re\{\partial_y^2 G_b\}$, the two effective dipoles will not resonate exactly at the same frequency, thus this value of the absorption maximum will

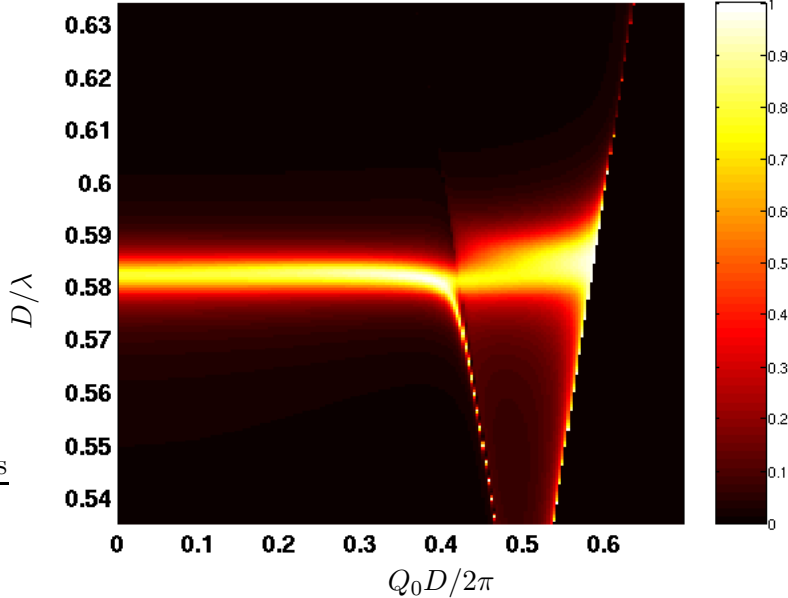


FIG. 3: (*p*-polarization) : Extinction map for an array of SiC cylinders with a period $D = 6.15 \mu m$, a radius of $a = 0.5 \mu m$. The localized surface phonon-polaritons resonance, at the wavelength $\lambda \simeq \lambda_P$, is isotropic.

be very sensible to the lattice parameters. Together with this condition, it can be easily shown that the other condition to reach the maximal absorption is $q_0 = Q_0(\theta = 45^\circ)$. We represent in Fig.2(e) and (f), respectively the absorption and extinction spectra of an array of SiC cylinders with a radius of $a = 0.5 \mu m$ and for an incident angle of $\theta = 45^\circ$ and several periods. Similarly to s-polarization, there are two kinds of resonances, (1) geometric resonance characterized by very sharp peaks at wavelengths close to Rayleigh frequencies, (2) a broader *double peak* at a wavelength $\lambda \simeq \lambda_P$. This double peak corresponds to the resonances of the *y*- and *x*-dipoles, (red or blue) shifted depending on the sign (+ or -) of $\partial_x^2 G_b$ and $\partial_y^2 G_b$. As discussed above, $\approx 100\%$ absorption takes place only when $\partial_x^2 G_b \approx \partial_x^2 G_b$. It is worth noticing that in the wavelength range where $\Re\{1/\alpha_p\} < 0$ (i.e. $|\epsilon| < 1$), there are no geometric resonances. This explains the anomalous shape of the LSPR extinction peak for $D = 6.15 \mu m$ (black bold solid line in Fig.2(f)), as the Rayleigh frequency ($\lambda = 10.5 \mu m$) lies in a range where $\Re\{1/\alpha_d\} \lesssim 0$. At this wavelength, we can just observe the (*y*-dipole) Rayleigh transparency dip in the extinction spectrum (see also Fig. 3). These results provide a simple and analytical explanation of the anomalous shape of the extinction peaks observed in recent numerical simulations [13].

In conclusion, this paper gives a simple analytical method to derive the optical properties of sub-wavelength cylinders arrays. We have shown that in s-polarization, absorption resonances can absorb up to half of the incident power. The absorption and extinction spectra for p-polarization presents a more complex structure due to the contribution of two orthogonal dipoles. It is remarkable that, as we have shown, by an appropriate choice of parameters a subwavelength cylinder array can become a perfect absorber. We believe that our analysis paves a new way for the nanoengineering of chemical and biological sensors and photo-thermal devices based on nanoparticle arrays.

We thank S. Albaladejo, J. García de Abajo and O. J. F. Martin for interesting discussions. This work has been supported by the Spanish MEC (Ref. No. EX2005-1181), the EU Integrated Project “Molecular Imaging” (EU contract LSHG-CT-2003-503259) and the EU network of excellence ”Plasmo-nano-device” (FP6-2002-IST-1-507879).

* URL: <http://www.uam.es/mole>

- [1] A.N. Shipway, E. Katz and I. Willner, *ChemPhysChem* **1**, 18 (2000).
- [2] J. P. Kottmann and O. J. F. Martin, *Phys. Rev. B*, **64**, 235402, (2001). J. P. Kottmann *et al.*, *Opt. Express* **6**, 213-219 (2000).
- [3] S.J. Oldenburg *et al.*, *Chem. Phys. Lett* **288**, 243 (1998).
- [4] J.-J. Greffet and M. Nieto-Vesperinas, *J. Opt. Soc. Am. A* **15**, 2735 (1998).
- [5] J.-J. Greffet *et al.*, *Nature (London)* **416**, 61 (2002).
- [6] M. Laroche *et al.*, *Opt. Lett.* **30**, 2623 (2005).
- [7] S.Y. Lin *et al.*, *Phys. Rev. B* **62**, R2243 (2000).
- [8] S. Enoch *et al.*, *Appl. Phys. Lett.* **86**, 261101 (2005).
- [9] M. Laroche, R. Carminati and J.-J. Greffet, *Phys. Rev. Lett.* **96**, 123903(2006).
- [10] V. Yannopapas, *Phys. Rev. B* **73**, 113108 (2006).
- [11] B. Lamprecht *et al.*, *Phys. Rev. Lett.* **84**, 4721 (2000). N. Felidj *et al.*, *Phys. Rev. B* **64**, 075419 (2002).
- [12] Q.-H. Wei *et al.*, *Nano Lett.* **4**, 1067 (2004).
- [13] S.Zou, N. Janel and G.C. Schatz, *J. Chem. Phys.*, **120**, 10871 (2004). E.M. Hicks *et al.*, *Nano Lett.* **5**, 1065 (2005).

- [14] M.S. Anderson, Appl. Phys. Lett **83**, 2964 (2003).
- [15] R. Gómez-Medina, M. Laroche and J.J. Sáenz, Opt. Express **14**, 3730 (2006).
- [16] Foldy L., Phys. Rev. **67**, 107 (1945).Lax M., Phys. Rev. **85**, 621 (1952).Twersky V., J. Opt. Soc. Am **52**, 145 (1962).K. Ohtaka and H. Numata, Phys. Lett. **73A**, 411 (1979).
- [17] R. Gómez-Medina and J.J. Sáenz, Phys. Rev. Lett. **93**, , 243602 (2004).
- [18] V.A. Markel, J. Chem. Phys., **122**, 097101 (2005).
- [19] M. Meier and A. Wokaun, P.F. Liao, J. Opt. Soc. Am. B **2**, 931 (1985).
- [20] E.D. Palik, *Handbook of Optical Constants of Solids* (Academic Press, San Diego, 1985).
- [21] F. J. García de Abajo, R. Gómez-Medina and J. J. Sáenz, Phys. Rev. E, **72**, 016608, (2005).
- [22] F. J. García de Abajo, and J. J. Sáenz, Phys. Rev. Lett. **95**, 233901 (2005).F. J. García de Abajo *et al.*, Opt. Express **14**, 7 (2006).